In vitro vascular anastomosis with a 1.9 micron laser and dissolvable albumin stents

Reid McCargar[1], Kari Jensen[2], Amanda Dayton[2],
Katrina Murphy[2], Hua Xie[2], Scott A. Prahl[2]

May 19, 2011

[1]Dept. of Electrical and Computer Engineering, Portland State University
[2]Oregon Medical Laser Center, Providence St. Vincent Medical Center, Portland, OR

Abstract

We present a clinically-relevant method for producing and sterilizing dissolvable albumin stents to provide intralumenal support in vascular anastomosis, and a method for photothermally welding vessels using a 1.9 μm diode laser with albumin solder and water as the chromophore. The axial tensile strength and burst pressure of welded vessels were tested *in vitro*. Optimized weld parameters yielded tensile strengths of 4.4±1.2 N and burst pressures of 400±90 mmHg with stay sutures. It was concluded that stay sutures would be necessary *in vivo* due to degradation of the tensile strength with exposure to moisture. Stent dissolution was monitored with UV absorbance measurements in PBS, which produced similar results when compared to measurements by weight in blood ($p = 0.99$). Sterilization by 25 kGy γ-irradiation did not cause significant changes ($p > 0.6$) in stent solubility, which was primarily volume-dependent. Under simulated intravascular flow conditions, 3 mm stents dissolved completely with 2.7±0.7 mL/mg.

1 Introduction

Creating vascular anastomosis with a laser was first reported [1] in 1979 and offered advantages over traditional suture such as an immediate watertight seal [2], reduced operative time [3–5], faster healing [6], and reduced intimal hyperplasia [7]. Tissue welding with an infrared ($\sim$800 nm) laser in combination with albumin solder containing indocyanine green (ICG) was used on blood vessels [8–10], the urinary tract [11], and skin [12, 13]. Higher albumin concentrations in the solder have been shown to increase tensile strengths [14, 15]. Despite these innovations, laser welding has not gained widespread clinical acceptance. The main disadvantages of the laser-assisted procedure are the low strength of the resulting anastomosis [2], especially in the acute healing phase up to 4 days postoperatively [16], and increased anastomotic pseudoaneurysm rate [3, 5, 6, 17]. As new innovations erode these barriers, laser anastomosis, whether accomplished photothermally or photochemically, becomes more surgically relevant.

In photochemical tissue bonding, tissue is fused by covalently cross-linking adjacent protein molecules. Two photo-activated dyes have been used: Rose Bengal (a xanthene dye) and naphthalimides. No work has been published on the naphthalimides for the last decade [18, 19] and no long term cell viability studies have been published despite early promise. Rose Bengal has been used successfully in acellular tissues [20–24], but inhibits chrondrocyte cell growth [25] and is absorbed intracellularly where mucus membranes have been compromised [26]. This illustrates a fundamental problem with photochemical processes: intracellularly absorbed dyes can cause covalent cross-linking within cells upon irradiation, and any residual reactive species that have not interacted are potential foci for later problems.

Concerns about the biocompatibility of thermally-denatured albumin are mitigated by the long history of the use of electrocautery. Albumin is present in whole blood at 35–

55 g/L [27] and bleeding is routinely stopped by thermally denaturing whole blood and surrounding tissue. Consequently, whenever electrocautery is used to stop bleeding, denatured albumin remains and has not caused problems with healing. However, if an exogenous dye like indocyanine green (ICG) is added to the albumin, then the degradation products of the dye may cause problems. The optical degradation products of ICG have been shown to have cytotoxic effects [28–30].

In this study, a compact diode laser (nLIGHT Corp., WA) operating at at 1.9 microns was chosen to match a strong absorption peak of water, thereby eliminating the need to add exogenous chromophores to the albumin. The 1.9 micron absorption band arises from a combination of bending of the H–O–H molecule and a stretching in OH. The absorption coefficient of water at this wavelength is roughly 7.7/mm which corresponds to a penetration depth of ∼130 microns. The 1.9 micron laser has two primary advantages over a 10.6 micron CO_2 laser, which is also strongly absorbed by water: 1.9 micron light is readily transmitted through a standard quartz optical fiber and only penetrates ∼15 microns, heating only the surface of the albumin. The 1.9 micron wavelength was first demonstrated for anastomosis by Kung *et al.*who used a modified Nd:YAG laser, a few years later using a diode laser by Mordon *et al.*, and more recently in human clinical trials by Leclère *et al.* [31–34].

Finally, dissolvable glyceride stents have been used to support vessel anastomosis during suturing and have have caused minimal ischemia [35, 36]. Dissolvable albumin stents with ICG have also been used in 800 nm laser-assisted welding of ureters and vessels [37–40]. In this work, we combine the use of the 1.9 micron laser with albumin stents and present *in vitro* effects of various welding parameters on mechanical properties of the anastomosis.

2 Materials and methods

2.1 Stent and solder production

2.1.1 Concentration of albumin

Human serum albumin (HSA) (Albuminar, CSL Behring, IL) was concentrated to 55.0–57.4% (all albumin concentrations expressed as w/w) by evaporation of water through 25 kDA molecular weight cutoff dialysis tubing (Spectra/Por, Spectrum Laboratories, CA) over 10–16 hours. This concentration method proved advantageous over our previous pressure filtration method [41] which was difficult to monitor, required extended continuous observation, failed to eliminate spatial concentration gradients, and often led to filter rupture.

During dialysis, the albumin concentration C_{HSA} was monitored by weighing the tubing assembly at regular intervals and calculating C_{HSA} based on the weight loss from the starting weight. Once the target concentration was reached, the dialysis tubing was removed and the concentrated albumin was vacuum sealed in a foil pouch. Radial concentration gradients were noted at this point because the outermost surface was much more rigid than the inner albumin. After sealed storage in the foil bags for 96 hours or more, the texture of the albumin was essentially homogenous. To verify these tactile observations, 3 core and 3 surface refractive index measurements were taken from 3 different cross sections of a cylinder of 55.4% HSA immediately after dialysis, then again from adjacent cross sections after 96 hours of sealed storage.

2.1.2 Extrusion, sectioning and stent characterization

A cylinder of concentrated albumin was inserted into a purpose-built, vise-mounted extruder. A set of dies with circular orifices ranging from 1.5–5.0 mm in 0.5 mm increments determined

the stent outer diameter, while concentric pins (0.7–2.7 mm) controlled the inner diameter. The die and pin with the desired stent dimensions were assembled and mounted on the extruder. A piston forced the concentrated albumin through the die. The extruded tube of albumin was collected on a sheet of rubberized Teflon to prevent curling or drooping and cut into 100 mm lengths with a razor blade. This process continued until all the concentrated albumin was extruded.

The 100 mm long albumin tubes were allowed to dry for 10–30 minutes at room temperature; at this point the tubes were firm enough to be cut without slumping. The albumin tubes were cut into 17 mm long stents by rolling back and forth gently under a scalpel edge. This cutting technique minimized the tendency of the stent to pinch shut. Finished stents were stored individually in 1.5 mL micro-centrifuge tubes. Each lot of stents was sealed in an aluminum pouch and (except for non-irradiated controls) γ-irradiated at 25–40 kGy (Steris, Isomedix, IL). The stents were stored at room temperature after sterilization.

Finished stents were viewed through a stereomicroscope (MZ-12, Leica, GMBH) to observe surface uniformity. To monitor the accuracy and precision of the dimensions, five stents were randomly selected from five extrusions of 3.0/1.1 to 4/2.7 stents with concentrations ranging from 55.0% to 57.4%. The outer diameter d_{outer} was measured with digital calipers (Absolute Digimatic, Mituyo Corp) and reported as percent change from the orifice diameter: $1 - d_{outer}/d_{orifice}$ where $d_{orifice}$ is the diameter of the die orifice.

2.2 Measuring albumin concentration

2.2.1 Measuring concentration by drying

To assess the extent of concentration changes taking place during extrusion and sectioning, nine 3/1.6 (outer diameter/inner diameter) stents with a pre-extrusion concentration of 55.4% were dehydrated completely in a convection oven at 50°C. The concentration was

determined by the ratio of the dry weight to packaged weight, measured to the nearest 0.1 mg (AE 200 Mettler Toledo, Inc). Stents were weighed after 96, 100, and 112 hours. Although simple and reliable, this method was inconvenient because significant non-recoverable quantities of albumin were required, and several days were required for complete dehydration at non-denaturing temperatures.

2.2.2 Measuring concentration by refractive index

A rapid, accurate, and less wasteful method of measuring the concentration of albumin using an Abbé refractometer (Fisher Scientific, Inc.) was developed. A calibration curve was generated using known concentrations of HSA. Refractive index measurements were taken prior to placing a drop on a glass slide and drying it out completely in a convection oven at 50°C. The total mass of albumin in solution m_{total} and the dehydrated mass m_{HSA} was linearly related to the index of refraction n at 23°C,

$$C_{HSA} = \frac{m_{HSA}}{m_{total}} = 459.28\,(n - 1.3317) \tag{1}$$

The index of refraction of water is 1.3317 and therefore pure water will have $C_{HSA} = 0$. The precision of this method is 0.01% over the range 0–60 % [42]. All measurements were made between 22 and 24°C.

2.2.3 Measuring concentration by ultraviolet absorption

Low concentrations (0–0.7 μg/mL) of albumin were measured by UV spectrophotometry. A calibration curve was prepared by dissolving 0.1, 0.2, and 0.3 mL aliquots of 22.35% HSA (determined by refractive index measurements) in 100 mL of phosphate-buffered saline (PBS) to produce concentrations of 0, 0.2235, 0.4470, 0.6705 μg/mL. The absorbance of each solution was measured once from 270–345 nm in a plastic cuvette (Plastibrand, GMBH) using

a spectrometer (Cary 100-Bio, Varian).

Plastic cuvettes have non-negligible absorption in the ultraviolet. This problem was corrected by subtracting the absorbance of a cuvette filled with PBS (no albumin). Variations caused by cuvette surface reflectivity were corrected by subtracting a constant value from all wavelengths. This constant was chosen so that the spectrum of a solution of albumin would be zero at 345 nm. A longer wavelength would have been better, but the spectrophotometer changes lamps at 350 nm and the correlation between ultraviolet and visible absorbance is inconsistent. The calibration solution absorbances were corrected for cuvette reflection and absorbance as, $C_{HSA} = (0.94 \cdot A_{278} - 2.27)\,\mu$g/mL, where A_{278} is the corrected absorbance at 278 nm.

2.3 Stent Dissolution

Stents were sterilized with γ-irradiation, because ethelene oxide sterilization alters them chemically, steam denatures them, and the high viscosity precludes filtration sterilization. It is known that γ-irradiation causes protein fragmentation and aggregation, altering chemical and physical properties [43–47]. The effect of γ-irradiation on stent solubility was investigated by monitoring stent dissolution without flow.

Spectrophotometric measurement of albumin concentration in PBS allowed for rapid and precise data collection, compared to monitoring weight changes of stents dissolved in blood. Dynamic dissolution tests were performed to compare solubility in PBS and blood, and to observe the effects of stent geometry and flow rate.

2.3.1 Static dissolution

Static dissolution rates were evaluated by immersing solid albumin cylinders in PBS. The cylinders were extruded using 56% (w/w) HSA with no inner lumen and sectioned to form 12–25 mm long solid cylinders with 2 mm outer diameters. The cylinders were weighed,

placed in polyethylene microcentrifuge tubes, divided into 2 equal-numbered groups, and vacuum sealed in foil pouches after purging with nitrogen. One group was γ-irradiated at 25–40 kGy, while the other was stored at room temperature. Each cylinder was dissolved in 5 mL PBS maintained at 37 °C in a disposable glass culture tube (Thermo Fisher Scientific, Inc.). At 100, 200, and 300 s intervals, three irradiated, and three non-irradiated sample tubes were decanted into empty culture tubes. The concentration in each tube was measured spectrophotometrically. The total amount of dissolved albumin was normalized to the initial surface area of the cylinder and reported in μg/mm^2.

2.3.2 Dynamic dissolution in blood

Dissolution coefficients were measured by pumping blood through stents at known flow rates. To approximate intravascular implantation, stents were inserted into a 30 mm long section of tubing with lumen diameter of 3.17 mm for the 3.0 mm outer diameter stents and 4.35 mm for the 4.0 mm outer diameter stents. Fluid was pumped through the stent for 5–20 minutes until the stent was completely dissolved. The fluid was kept at 37°C and recirculated through the tubing for 20 minutes prior to dissolution to ensure uniform temperature throughout the system. It was not recirculated after beginning the dissolution.

In citrated whole porcine blood, dissolution progress was monitored by weighing the stent-containing section of tubing before after ten seconds, and then at 30-second intervals. Flow was stopped before disconnecting the tubing section, which was quickly rinsed with 2 mL of ice water and shaken to remove trapped liquid before weighing. Each stent was used for only one weight measurement, and 3 stents were measured per time point. Seventeen stents were used to measure dissolution progress over 2.5 minutes of flow. The dissolution coefficient, V_{blood}^{diss}, representing the volume required for stent dissolution per unit mass, was and calculated in mL/mg using the expression

$$V_{blood}^{diss} = \frac{\Delta V}{\Delta m} \tag{2}$$

where Δm is the change in stent weight observed for the solvent volume ΔV passed through the stent.

2.3.3 Dynamic dissolution in PBS

PBS dissolution coefficients were obtained with the same pump and tubing configuration used to measure dissolution coefficients in blood (after thorough cleaning and cycling with PBS at 37°C for 20 minutes). For each stent, the eluent was collected in cuvettes for UV absorbance measurement after ten seconds, and then at 30 second intervals. Flow was not interrupted during the dissolution. When it became apparent that dissolution depended primarily on the solvent volume passed through the stent, the fraction of the stent remaining $f(V)$ was expressed as a function of volume, rather than time:

$$f(V) = \frac{A_{278\,nm}^{(V)}}{A_{278\,nm}^{max}} \tag{3}$$

where $A_{278\,nm}^{(V)}$ is the corrected absorbance for the volume V, and $A_{278\,nm}^{max}$ is the highest absorbance measured in each dissolution. $A_{278\,nm}^{max}$ occurred at 10 and 30 s in all tests. The dissolution coefficient (in mL/mg), was reported as the solvent volume $V_{10\%}$ corresponding to $f(V)$=0.1, divided by 90% of the initial mass of the stent m_0:

$$V_{PBS}^{diss} = \frac{V_{10\%}}{0.9\, m_0} \tag{4}$$

All tests comparing blood and PBS were performed with a flow rate of 139 mL/min on 3.0/1.6 stents. The solubility of 3.0/1.6 stents was measured at PBS flow rates ranging from 27–139 mL/min. Another series of tests comparing the effect of wall thickness on solubility

was performed in PBS on 4.0 mm outer diameter stents with inner diameters of either 1.1 or 2.7 mm at 100 mL/min.

2.4 *In vitro* mechanical assessments

2.4.1 Anastomosis

Domestic porcine carotid arteries (Animal Technologies, TX and Sierra Medical Technologies, CA) were harvested into PBS and shipped overnight on ice. All had inner diameters of approximately 4 mm. Vessels were selected at random and sectioned into 3 cm lengths for tensile strength testing, and into 5 cm lengths for burst pressure testing.

Vessels were welded under magnification by a stereoscope (SZ-STB1, Olympus Corp) using albumin solder externally and albumin stents internally to provide internal support. Excess fascia and adventitial tissue were first cut away, and excess moisture was dabbed away with a paper tissue. The vessel was transected with surgical scissors at a right angle. A stent was inserted into the cut end of each vessel, and the ends were drawn into close and uniform contact over the stent. The outer diameter of the stent was chosen to match the vessel inner diameter such that it could be inserted with only slight pressure, but would not slip out under light manipulation during welding.

Albumin solder was then applied to the anastomosis with a 1.0 mL syringe and a 27 Ga needle. For $C_{HSA} \leq 43\%$ (w/w), solder surface tension was low, so minimal manual spreading was necessary to achieve uniform coverage. The solder was denatured with 1.9 micron laser light until a uniform golden-tan color change was observed. A green LED coupled to the laser fiber provided a visible aiming beam. Procedure time was measured as the time from vessel transection to weld completion. Irradiation time was measured as the time the laser was activated, but does not account for small periods of time to reposition the laser spot on the vessel.

Laser spot size was dependent on the focus length, and differed from the aiming beam spot size due to dispersion. A nominal minimum spot size of 0.2 mm at 1.9 microns was measured using laser alignment paper (Zap-It Corp.) with the handpiece 2 mm past the aiming beam focus length. The nominal minimum spot size was used for all anastomoses.

Vessels were immediately placed in sealed polyethylene centrifuge tubes with PBS-moistened paper tissues to prevent dessication and kept at 4°C until mechanical strength testing. Five vessels were welded for each set of weld parameters (except 1 mm wide weld tensile tests, where $N = 7$). Welding parameters were independently varied to discern the optimal parameters. Weld width was varied from 1–3 mm; solder concentration from 22–46% HSA (w/w); laser power from 430–610 mW; and the number of solder layers from 1–3.

Ten vessels were welded with four interrupted 6–0 prolene stay sutures evenly spaced around the anastomosis. To determine if prolonged exposure to moisture degraded the anastomosis, vessels were welded with the most surgically-promising parameters (judged by low weld time, high strength, and reproducibility) and stored submerged in PBS at 4°C for 0 and 5 hours before burst and tensile testing. Five vessels with sutures only, as in conventional surgical application, were burst and tensile tested for comparison.

2.4.2 Tensile strength

Axial tensile strength testing was performed for all combinations of weld parameters using an 858 Mini Bionix II (MTS Systems, MN) materials tester. Before mounting in the materials tester, 100 mL PBS was passed through the vessel to dissolve the stent. Vessels were anchored on both sides of the weld with aluminum clips and pulled apart at 2 mm/s. The tension was measured with a calibrated gauge (661.11A.02, MTS Systems) and recorded using the software controller for the MTS. The maximum tension for each vessel prior to breaking was recorded.

2.4.3 Burst Pressure

The output of a pressure transducer (68074-12, Cole-Parmer Inc., IL) precalibrated to produce 25 mV/mmHg was sampled at 15 Hz and digitally recorded (BNC 2120, National Instruments Corp). One-eighth inch barbed tube fittings were inserted into opposite ends of the vessel and were tied down tightly with 1/8″ wide umbilical tape. The inlet tube fitting was connected to a peristaltic pump (505Di, Watson-Marlow Inc., MA) drawing from a reservoir of PBS at 23°C. The outlet tube fitting was connected to a T-section with the pressure transducer and a stopcock which could be closed or opened to build or relieve pressure. With the stopcock closed, PBS was pumped into the vessel section until bursting. Burst pressure was reported as the difference between ambient and maximum pressure before bursting.

2.5 Statistical analysis

Margins were reported as ± one standard deviation from the mean. One-way analysis of variance (ANOVA) was used to compare means. Post-hoc analysis was performed with Bonferroni's method.

3 Results

3.1 Stent Fabrication

3.1.1 Albumin concentration accuracy and precision

Refractive index measurements taken immediately after dehydration showed a core concentration of 47.26±0.04%, and a surface concentration of 60.2±0.4%. The average concentration was 55.4%. Refractive index measurements from adjacent cross-sections after 96 hours of sealed storage reflected an average core concentration of 56.7±0.4%, and an average surface concentration of 59±3%. Minimal variation in concentration indicators (opacity, friability,

and slumping) was observed after post-dialysis storage in substantial excess of 96 hours.

3.1.2 Accuracy and Precision of Stent Production

Measurement of stent outer diameters revealed that the extrudate had a tendency to shrink by 5±3%. Only one of the 25 stents measured had a larger outer diameter than the die orifice, presumably because it encountered mild compression while exiting the die.

Magnified observation revealed that stents made with $C_{HSA} < 55.5\%$ deformed under light mechanical stress and developed deep cracks when sectioned after drying; the dry stents tended to break into large pieces on light handling. Stents made from slightly higher albumin concentrations (56.5±0.5%) did not deform under light mechanical stress and could still be bent under moderate pressure, especially if warmed slightly (i.e., by a surgeon's hands to accommodate a curved anastomosis site) without causing cracks or lumenal collapse. Concentrations above 57.0% required considerably more force to extrude and these stents did not deform under light mechanical stress. Shallow surface cracks became discernible immediately after exiting the die, and small ($\sim 10\,\mu$m thick) sheets flecked off. Deep cracks were not observed, nor did stents break into large pieces. Small $\sim 10\,\mu$m longitudinal striations were observed at all extrudate concentrations.

Magnified observation of inner lumen surfaces after dividing stents longitudinally revealed inner surfaces with similar properties to outer surfaces. No closure or narrowing of the inner lumen was observed for 55.5–57.4% extrudate concentrations.

3.2 Dissolution

3.2.1 Static dissolution comparing γ-irradiated and non-irradiated stents

Dissolved albumin concentrations increased from 60 μg/mm^2 after 100 seconds to 140 μg/mm^2 after 300 seconds for both irradiated and control stents (Fig. 1). Average dissolution rates

were 0.5±0.1 and 0.5±0.2 μg/mm^2/s, respectively. The dissolution rate is given as the mass of albumin dissolved into solution per second, normalized over the original surface area of the cylinder.

[Figure 1 about here.]

3.2.2 Dissolution in Blood and PBS

For dissolution times less than 1 minute in blood, it was difficult to remove excess liquid held in the small inner lumen before weighing the tubing section. This was apparent in the large variations in the dissolution times (Fig. 2, Table 1).

[Figure 2 about here.]

The standard deviation was more than five times higher in blood than in PBS. Absorbance measurement was also ∼10 times faster.

3.2.3 Dissolution of 3.0/1.6 stents at different flow rates in PBS

As the flow rate decreased, the time to reach 10% of A^{max} increased from 111 s at 139 mL/min to 495 s at 27 mL/min. Plotting C_{HSA} against volume rather than time suggested that stent dissolution depended primarily on total solvent volume regardless of flow rate (Fig. 3, Table 1). $\frac{A^{(V)}}{A^{max}}$ decreased to a common baseline after approximately 236 mL had passed through the stent. No stent required more than 4.2 mL/mg to reach 10 % of A^{max}.

[Figure 3 about here.]

3.2.4 Dissolution for different inner lumen diameters

Dissolution coefficients ranged from 2.0 to 2.6 mL/mg, with no clear or significant trends arising as a function of wall thickness. The average dissolution volume over all wall thick-

nesses was 2.2±0.5 mL/mg, with no stent requiring more than 3.2 mL/mg to reach 10% of peak absorbance (Table 1).

[Table 1 about here.]

3.3 *In vitro* mechanical assessments

Vessels with 1–7 mm wide welds (2 layers of 38% HSA, 430 mW laser power) had average ultimate tensile strengths of 0.6±0.1 N to 0.7±0.3 N (Fig. 4), with 3 mm vessels performing best. Average burst pressures were 13±23 to 150±45 mmHg (Fig. 5), with 3–5 mm welds performing comparably and better than other widths. Three vessels with 1 mm welds, and 2 vessels with 7 mm welds developed holes or separated completely while mounting on the tube fittings for burst testing. No vessels with 3 or 5 mm welds failed in such a premature fashion. Irradiation time increased linearly from 7 to 17 minutes as weld width increased from 1 to 7 mm. Faster anastomoses than those reported here have been achieved in studies currently underway with larger spot sizes and higher powers.

[Figure 4 about here.]

[Figure 5 about here.]

Increasing solder concentration (with $P = 430$ mW, $W = 3$ mm, and $n_{layers} = 2$) led to increases in ultimate tension from 0.5±0.2 N at 22% to 1.3 ±0.5 N at 43%. At 46%, average tensions decreased slightly to 1.1±0.9 N (Fig. 4). Delamination occurrence and relative standard deviation increased above 38%. All $C_{solder} \leq 38\%$ welds failed by tearing through the denatured albumin sheath, while 20% of 43% welds, and 80% of 46% welds failed by delamination, indicating less consistent adhesion to the vessel than at lower concentrations.

Tensile strengths increased from 0.6±0.5 to 1.4±0.5 N as the number of layers increased from 1–3 (with $W = 3$ mm, $C_{solder} = 38\%$, and $P = 430$ mW) (Fig. 4). Procedure time also increased linearly from 5 to 9 minutes.

Welds made with laser powers of 430–610 mW ($n_{layers} = 2$, $W = 3$ mm, $C_{solder} = 38\%$) had average tensile strengths of 0.8±0.1 to 2.2±0.9 N, with 570 mW yielding the highest strength (Fig. 4). Counter to expectations, increasing laser power did not significantly reduce the irradiation time.

[Table 2 about here.]

If the anastomosed vessels were submerged in PBS for five hours, maximum tension for $C_{solder} = 38\%$, $P = 570$ mW, $W = 3$ mm, $n_{layers} = 2$ sutureless welds decreased from 2.1±0.9 N to 0.3±0.2 N, indicating that vessels welded without stay sutures would not retain adequate tensile strength *in vivo*. With the addition of 4 stay sutures, average maximum tension still decreased from 4.4±0.8 N to 3.3±0.6 N after storage (Fig. 6 top, Table 2). Burst pressure averages in welded, stay-sutured vessels did not decrease significantly ($p = 0.8$) after storage in PBS, but the standard deviation increased from 86 to 388 mm Hg (Fig. 6 top). Although the denatured albumin cuff at the anastomosis did not dissolve in PBS, it swelled visibly and became more friable.

[Figure 6 about here.]

4 Discussion

4.1 Stent production

Measurements indicated the extrusion orifice needed to be 5% larger than the target diameter to account for shrinkage, with ±7% precision in outer diameter of target. Owing to the elasticity of vascular tissue, this extrusion method exceeded the ∼250 μm resolution necessary for good stent fit.

96 hours of sealed storage was effective in reducing radial concentration gradients, and few (<1%) unsatisfactory stents were produced when pre-extrusion storage times greatly

exceeded 96 hours. No attempts were made to discern the minimum time required to reduce concentration gradients to less than 0.5%.

4.2 Stent dissolution

Differences in the static dissolution coefficients of γ-irradiated and non-irradiated stents were not significant ($p = 0.6$). The same average (2.7 mL/mg) dissolution coefficient was observed in dynamic dissolution tests in PBS and in blood. Insignificant differences (p=0.99) were found between stents dissolved in blood and PBS (Table 1).

Volume-dependent dissolution was observed with flow rates of 27–139 mL/min on 3/1.6 stents. Differences in dissolution volumes were not significant ($p > 0.3$) for any comparison of flow rates. Differences were not significant ($p > 0.7$) between any 4/x stents with varied inner diameter. Likewise, insignificant differences ($p > 0.5$) were observed when comparing 4/x and 3/x stent dissolution.

4.3 Weld mechanical properties

The tensile strength of vessels welded varied with weld width, laser power, and weld layers showed unequal variances, and post-hoc comparisons were not made. Although $C_{solder} = 43\%$ produced significantly higher tensile strengths than stock 22% albumin ($p = 0.045$), differences between higher solder concentrations were not significant. High deviations (35% rel. at $C_{solder} = 43\%$, compared to 16% rel. at $C_{solder} = 38\%$) obscured the ideal solder concentration. Similarly, more solder layers improved tensile strength, but necessarily increased procedure time. Only weld width and the number of solder layers significantly affected irradiation time. The 3 mm wide welds produced the highest tensile strength, and burst pressures comparable to 5 mm welds.

Optimization efforts focused on achieving high tensile strength became irrelevant after

demonstrating that exposure to moisture significantly and substantially (∼85%) degraded the tensile strength of vessels without stay sutures. Although the decrease in average tensile strength was much smaller (∼24%) in welded vessels with stay sutures (Table 2), it was not statistically significant ($p = 0.198$).

Contrary to expectations following tensile testing, average burst pressures in stay-sutured vessels were higher after 5 hours in PBS than before, although the differences were not statistically significant. Welded and stay sutured vessels had substantially higher average burst pressures befor and eafter storage (Table 2). However, the differences were not significant due to high variation in all groups. The results do not strongly suggest that the burst pressure improvements are negated by exposure to moisture.

5 Conclusion

It has been shown that dissolvable albumin stents can be produced accurately and precisely by dialysis concentration and extrusion through a simple die at room temperature. These stents can be sterilized by gamma irradiation without decreasing their solubility. Owing to their fast, primarily volume-dependent dissolution, and their established biocompatibility, these stents can be used to provide internal support in laser anastomosis.

Although welding with albumin solder and a 1.9 μm laser resulted in poor tensile strength without the use of stay sutures, improvements in burst pressure were realized in laser-welded vessels compared to sutured vessels. The potential improvements in burst pressure and operative time warrant *in vitro* investigation.

Acknowledgements

We would like to acknowledge support by Air Force STTR-AF07-T033 and the help of Dennis McCal and Kirk Price from nLIGHT.

References

[1] Jain RK. Transient temperature distributions in an infinite, perfused medium due to a time-dependent, spherical heat source. J Biomechanical Engineering 1979; 101:82–86.

[2] Bass LS, Treat MR. Laser tissue welding: A comprehensive review of current future clinical applications. Lasers Surg Med 1995; 17:315–349.

[3] Serure A, Withers EH, Thomsen S, Morris J. Comparison of carbon dioxide laser-assisted microvascular anastomosis and conventional microvascular sutured anastomosis. Surg Forum 1983; 34:634–636.

[4] Frazier OH, Painvin A, Morris JR, Sharon T, Neblett CR. Laser-assisted microvascular anastomosis: angiographic and anatomopathologic studies on growing microvascular anastomosis: Preliminary report. Surgery 1985; 97:585–589.

[5] McCarthy WJ, LoCicero J, Hartz RS, Yao JST. Patency of laser-assisted anastomosis in small vessel: One-year follow-up. Surgery 1987; 102:319–325.

[6] Vale BH, Frenkel A, Trenka-Benthin S, Matlaga BF. Microsurgical anastomosis of rat carotid arteries with the CO_2 laser. Plast Reconstr Surg 1986; 77:759–766.

[7] Quigley MR, Bailes JE, Kwaan HC, Cerullo LJ, Block S. Comparison of myointimal hyperplasia in laser assisted and suture anastomosed arteries. J Vasc Surg 1986; 4:217–219.

[8] Oz MC, Chuck RS, Johnson JP, Parangi S, Bass LS, Nowygrod R, Treat MR. Indocyanine green dye enhanced vascular welding with the near infrared diode laser. Vasc Surg 1990; 24:564–570.

[9] Weng G, Williamson WA, Aretz HT, Pankratov MM, Shapshay SM. Diode laser activation of indocyanine green dye-enhanced albumin for *in vitro* internal mammary artery anastomosis. Lasers Surg Med 1994; 6:57.

[10] Sorg BS, Welch AJ. Laser-tissue soldering with biodegradable polymer films *in vitro*: film surface morphology and hydration effects. Lasers Surg Med 2001; 28:297–306.

[11] Kirsch AJ, Miller MI, Chang DT, Olsson CA, Hensle TW, Conner JP. Laser tissue soldering in urinary tract reconstruction: first human experience. Urology 1995; 46:261–266.

[12] Kirsch AJ, Chang DT, Kayton ML, Libutti SK, Treat MR, Hensle TW. Laser welding with albumin-based solder: experimental full-tubed skin graft urethroplasty. Lasers Surg Med 1996; 18:225–230.

[13] Cooper CS, Schwartz IP, Suh D, Kirsch AJ. Optimal solder and power density for diode laser tissue soldering (LTS). Lasers Surg Med 2001; 29:53–61.

[14] Wright EJ, Schlossberg SM, Poppas DP. Evaluation of optimal laser wavelengths and albumin solder concentrations for laser tissue welding (abstract 373). Lasers Surg Med 1995; 17.

[15] Poppas DP, Wright EJ, Guthrie PD, Shlahet LT, Retik AB. Human albumin solders for clinical application during laser tissue welding. Lasers Surg Med 1996; 19:2–8.

[16] Stewart RB, Benbrahim A, LaMuraglia GM, Rosenberg M, L'Italien GJ, Abbott WM, Kung RTV. Laser assisted vascular welding with real time temperature control. Lasers Surg Med 1996; 19:9–16.

[17] Quigley MR, Bailes JE, Kwaan HC, Cerullo LJ, Brown JT. Aneurysm formation after low power carbon dioxide laser-assisted vascular anastomosis. Neurosurgery 1986; 18:292–299.

[18] Judy MM, Matthews JL, Boriack RL, et al. Photochemical cross-linking of proteins with visible-light-absorbing naphthalimides. In: Proc. SPIE, volume 1882 1993, 1993:221.

[19] Judy MM, Fuh L, Matthews JL, et al. Gel electrophoresis studies of photochemical cross-linking of type I collagen with brominated-naphthalimide dyes and visible light. In: Proc. SPIE, volume 2128 1994, 1994:506.

[20] Chan BP, Kochevar IE, Redmond RW. Enhancement of porcine skin graft adherence using a light-activated process. J Surg 2002; 108:77.

[21] Mulroy L, Kim J, Wu I, et al. Photochemical keratodesmos for repair of lamellar corneal incisions. Invest Ophthal Vis Sci 2000; 41:3335.

[22] Proano CE, Mulroy L, Jones E, et al. Photochemical keratodesmos for bonding corneal incisions. Invest Ophthal Vis Sci 2004; 45:2177.

[23] Chan BP, Amann C, Yaroslavsky AN, Title C, Smink D, Zarins B, Kochevar IE, Redmond RW. Photochemical repair of achilles tendon rupture in a rat model. J Surg Res 2005; 124:274–9.

[24] Kamegaya Y, Farinelli WA, Vila Echague AV, Akita H, Gallagher J, Flotte TJ, Anderson RR, Redmond RW, Kochevar IE. Evaluation of photochemical tissue bonding for closure of skin incisions and excisions. Lasers Surg Med 2005; 37:264–70.

[25] Ibusuki S, Halbesma GJ, Randolph MA, Redmond RW, Kochevar IE, Gill TJ. Photochemically cross-linked collagen gels as three-dimensional scaffolds for tissue engineering. Tissue Eng 2007; .

[26] Feenstra RPG, Tseng SCG. What is actually stained by rose bengal? Arch Ophthalmol 1992; 110:984–993.

[27] Herrmann FR, Safran C, Levkoff SE, Minaker KL. Serum albumin level on admission as a predictor of death, length of stay, and readmission. Archives of Internal Medicine 1992; 152:125–130. PMID: 1728907.

[28] Matsui H, Karasawa Y, Sato T, Kanno S, Nishikawa S, Okisaka S. [Toxicity of indocyanine green dye on Mller cells]. Nippon Ganka Gakkai Zasshi 2007; 111:587–593.

[29] Engel E, Schraml R, Maisch T, Kobuch K, Konig B, Szeimies RM, Hillenkamp J, Baumler W, Vasold R. Light-induced decomposition of indocyanine green. Invest Ophthalmol Vis Sci 2008; 49:1777–1783.

[30] Sato T, Ito M, Ishida M, Karasawa Y. Phototoxicity of indocyanine green under continuous fluorescent lamp illumination and its prevention by blocking red light on cultured M"ller cells. Invest Ophthalmol Vis Sci 2010; 51:4337–4345.

[31] Kung RT, Stewart RB, Zelt DT, L'Italien GJ, LaMuraglia GM. Absorption characteristics at 1.9 microns: effect on vascular welding. Lasers Surg Med 1993; 13:12–17.

[32] Mordon SR, Martinot V, Mitchell V. End-to-end microvascular anastomoses with a 1.9-μm diode laser. Journal of Clinical Laser Medicine Surgery 1995; 13:357–361.

[33] Mordon SR, Schoofs M, Martinot VL, Capon A, Buys B, Patenotre P, Pellerin PN. 1.9-μm diode-laser-assisted anastomoses (LAMA) in reconstructive microsurgery: results of the preliminary clinical study. In: Anderson RR, et al., eds., Lasers in Surgery:

Advanced Characterization, Therapeutics, and Systems XI, volume 4244. SPIE 2001, 2001:272–279.

[34] Leclère FM, Schoofs M, Buys B, Mordon SR. Outcomes after 1.9 μm diode laser-assisted anastomosis in reconstructive microsurgery: results in 27 patients. Plast Reconstr Surg 2010; 125:1167–1175.

[35] He F, Tang NX. Stent assisted laser welding in a rabbit model. Med J PLA 1994; 19:383–385.

[36] He F, Wei L, Lanzetta M, Owen ER. Assessment of tissue blood flow following small artery welding with an intraluminal dissolvable stent. Microsurgery 1999; 19:148–152.

[37] Xie H, Shaffer BS, Prahl SA, Gregory KW. Intraluminal albumin stent assisted laser welding for ureteral anastomosis. Lasers Surg Med 2002; 31:225–229.

[38] Xie H, Shaffer BS, Prahl SA, Gregory KW. Laser ureteral anastomosis using intraluminal albumin stent in a porcine model. Lasers Surg Med 2003; 32:294–298.

[39] Xie H, Bendre SC, Gregory KW, Furnary AP. Laser-assisted end-to-end vascular anastomosis of elastin heterograft to carotid artery with an albumin stent in vivo. Photomed Laser Surg 2004; 22:298–302.

[40] Xie H, Bendre SC, Burke AP, Gregory KW, Furnary AP. Laser-assisted vascular end to end anastomosis of elastin heterograft to carotid artery with an albumin stent: a preliminary in vivo study. Lasers Surg Med 2004; 35:201–205.

[41] Moffitt TP, Baker DA, Kirkpatrick SJ, Prahl SA. Mechanical properties of coagulated albumin and failure mechanisms of liver repaired with the use of an argon-beam coagulator with albumin. Journal of Biomedical Materials Research 2002; 63:722–728.

[42] La Joie EN, Barofsky AD, Gregory KW, Prahl SA. Patch welding with a pulsed diode laser and indocyanine green. Laser Med Sci 1997; 12:49–54.

[43] Alexander P, Hamilton LDG. Irradiation of proteins in the solid state: III. Influence of oxygen and absorbed water on changes produced in bovine serum albumin. Radiation Research 1961; 15:193–201.

[44] Beauregard G, Potier M. Temperature dependence of the radiation inactivation of proteins. Analytical Biochemistry 1985; 150:117–120.

[45] Miekka SI, Forng R, Rohwer RG, MacAuley C, Stafford RE, Flack SL, MacPhee M, Kent RS, Drohan WN. Inactivation of viral and prion pathogens by gamma-irradiation under conditions that maintain the integrity of human albumin. Vox Sanguinis 2003; 84:36–44.

[46] Bowes JH, Moss JA. The effect of gamma radiation on collagen. Radiation Research 1962; 16:211–223.

[47] Benson RS. Use of radiation in biomaterials science. Nuclear Instruments and Methods in Physics Research Section B Beam Interactions with Materials and Atoms 2002; 191:752–757.

List of Figures

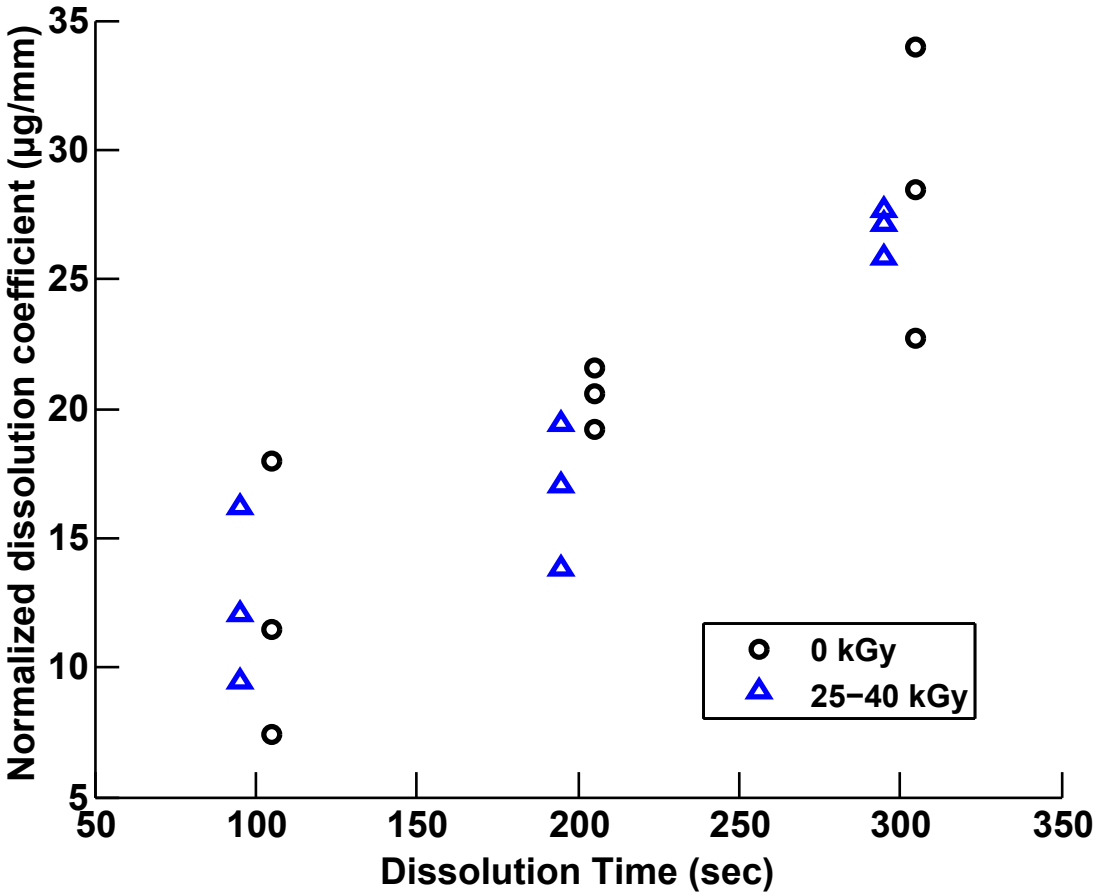

Figure 1: μg HSA dissolved, normalized over surface area vs. time in static dissolution comparing γ-sterilized and control stents in PBS without flow. Irradiated and non-irradiated data points were offset -5 and $+5$ sec., respectively for clarity. Differences in solubility were not significant at any time point.

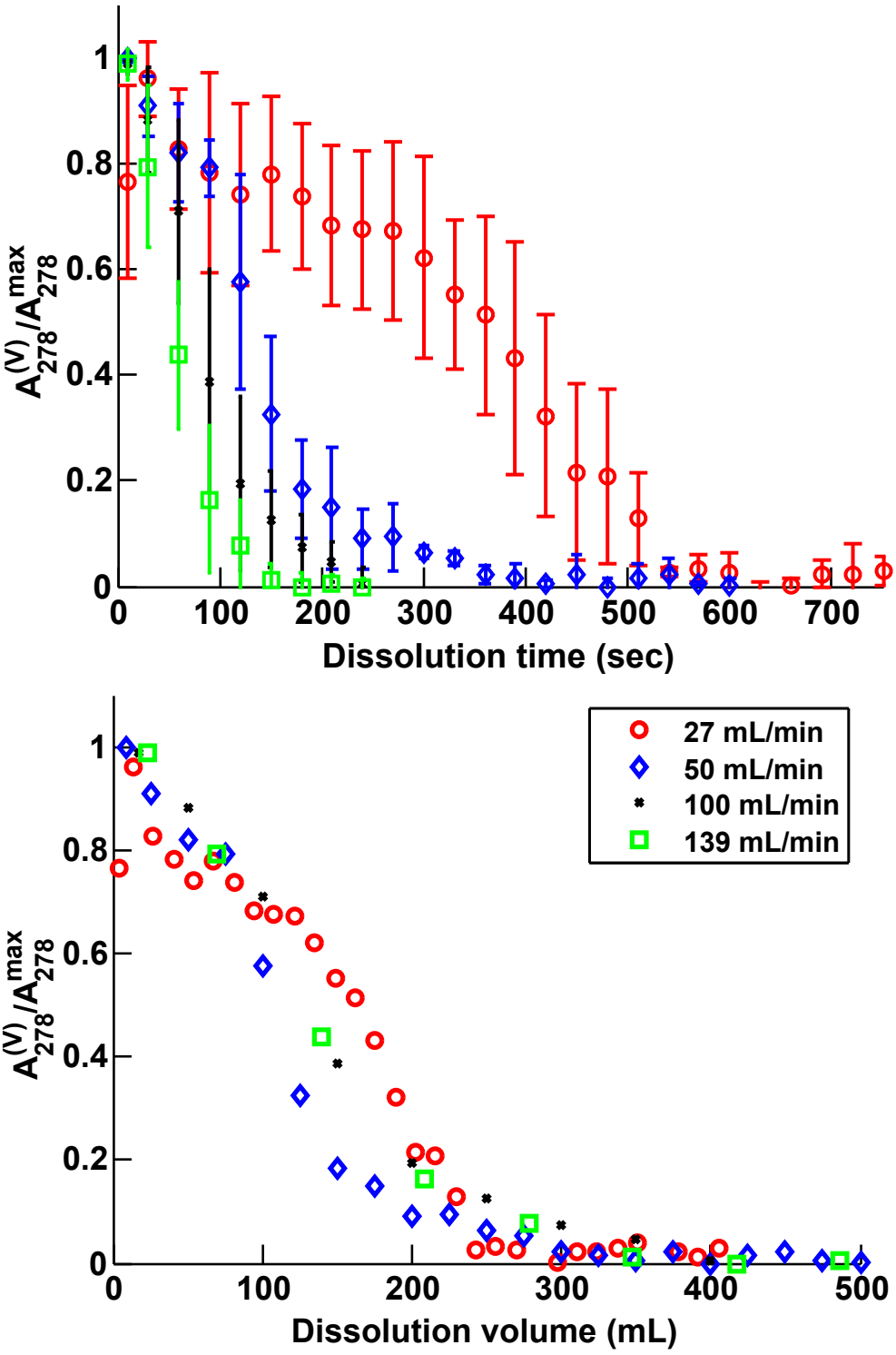

Figure 2: A_{278}/A_{278}^{max} vs. time (top), and A_{278}/A_{278}^{max} vs. volume (bottom) for 3 mm outer diameter stents (with different lumen diameters) in flowing PBS. Error bars represent one standard deviation, and some have been omitted for clarity. Flow rate did not significantly affect normalized dissolution as a function of volume ($p > 0.15$).

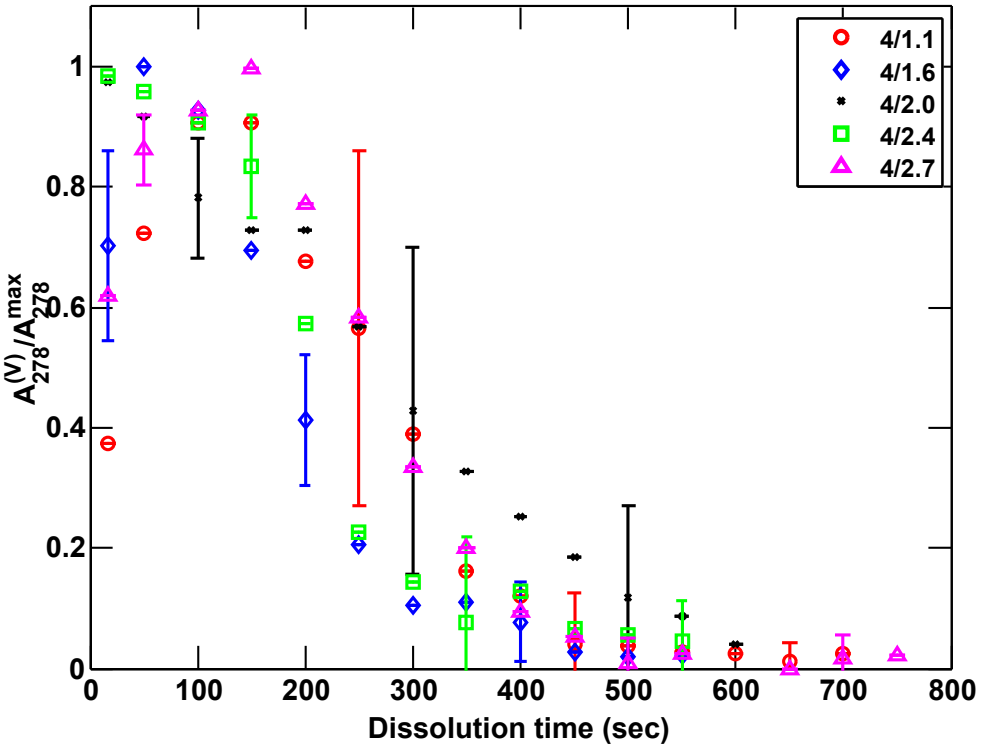

Figure 3: $A_{278\,nm}/A_{278\,nm}^{max}$ vs. volume for 4 mm outer diameter stents with varied inner lumen diameters. Some error bars (representing 1 standard deviation) have been omitted for clarity. No statistically-significant difference ($p > 0.45$) was observed as a function of inner lumen diameter.

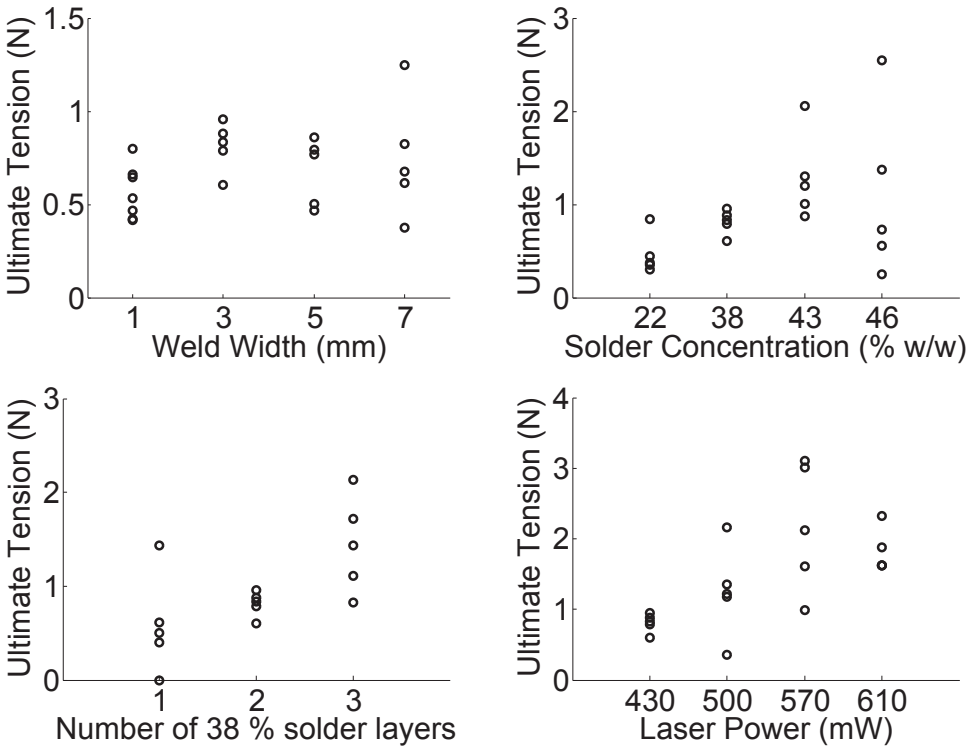

Figure 4: Maximum tension before breaking of (clockwise from upper left) vessels with varied welds widths; varied solder concentrations; varied laser powers; and varied solder layers. $N = 7$ for the $W = 1\,\text{mm}$ weld width test and $N = 5$ for all others.

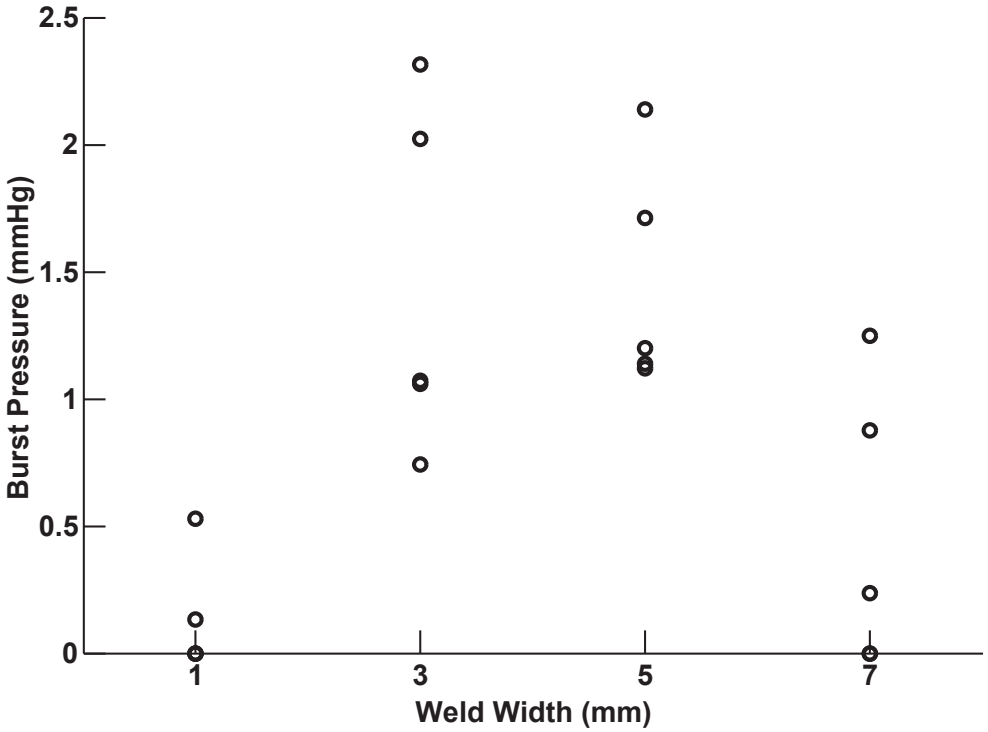

Figure 5: Burst pressure vs. weld width where $P = 430\,mW$, $n_{layers} = 2$, $C_{solder} = 38\%$. $N = 5$ for all points, except for $W = 7$, where $N = 4$ because a sensor I/O error occurred during testing.

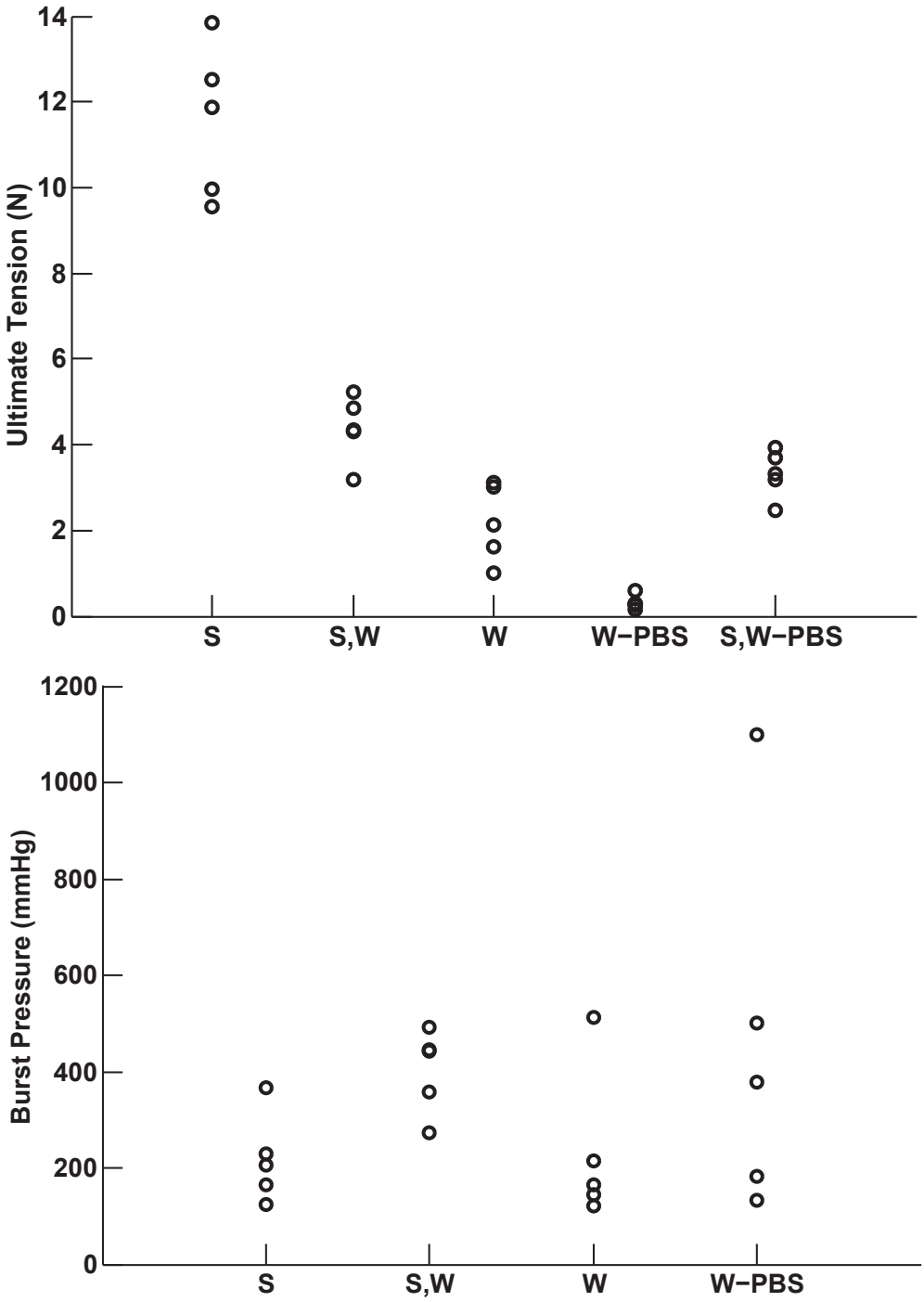

Figure 6: Tensile strength and burst pressure for vessels with sutures only (S), 4 stay sutures and welded albumin (S,W), and vessels welded without sutures (W). After storage in PBS, vessels with stay sutures retained tensile strength and pressure-holding capacity, while vessels without stay sutures lost significant tensile strength. Welds were 3 mm wide and used 2 layers of 38% (w/w) solder denatured at 570 mW.

List of Tables

Test Condition	(N)	Dissolution Coefficient (mL/mg)
blood	17	2.7±4.3
PBS	5	2.7±0.8
27 mL/min	3	2.7±0.4
50 mL/min	4	2.3±0.4
100 mL/min	5	1.9±0.5
139 mL/min	5	2.7±0.8
0.65 mm wall	4	2.1±0.5
1.45 mm wall	4	2.6±0.6
3/1.6	17	2.3±0.6
4/x	17	2.2±0.5

Table 1: Dissolution coefficient comparison from dynamic dissolution tests examining the effects of solvent, flow rate, and stent geometry. All tests at different flow rates were performed on 3/1.6 stents, while all tests comparing different wall thicknesses were performed on 4/x stents at a flow of 100 mL/min. No significant differences were found between groups

Group	Soaked in PBS	Tensile Strength (N)	Burst Pressure (mmHg)
Only Weld	no	2.1±1.0*	231±161
Only Weld	yes	0.3±0.2*	–
Continuous Sutures	no	11.6±1.8*	217±92
Welded + 4 Sutures	no	4.4±0.7	402±87
Welded + 4 Sutures	yes	3.3±0.6	458±388

Table 2: Vessels with only continuous sutures, only welds, and welds with 4 stay sutures were tested for tensile strength and burst pressure at the anastomosis. Some cases were submerged in PBS for hours prior to testing. Asterisks denote statistically-significant difference compared to welded + 4 suture samples.